https://doi.org/10.5194/egusphere-2022-1505
Preprint. Discussion started: 5 January 2023

Considerations for hypothetical carbon dioxide removal via alkalinity addition in the Amazon River watershed

Linquan Mu, Jaime B. Palter, Hongjie Wang

Graduate School of Oceanography, University of Rhode Island, Narragansett, RI, 02882, USA

Correspondence to: Linquan Mu (mulinquan@gmail.com)

Abstract. The Amazon River plume plays a critical role in shaping the carbonate chemistry over a vast area in the western tropical North Atlantic. We explore a thought experiment of ocean alkalinity enhancement (OAE) via hypothetical quicklime addition in the Amazon River watershed, examining the response of carbonate chemistry and air-sea carbon dioxide flux to the alkalinity addition. Through a series of sensitivity tests, we show that the detectability of the OAE-induced alkalinity increment depends on the perturbation strength (or size of the alkalinity addition, ΔTA) and the number of samples: there is a 90% chance to meet a minimum detectability requirement with ΔTA > 15 μmol kg^{-1} and sample size > 40, given background variability of 15–30 μmol kg^{-1}. OAE-induced pCO_2 reduction at the Amazon plume surface would range between 0–25 μatm when ΔTA = 20 μmol kg^{-1}, decreasing with increasing salinity. Adding 20 μmol kg^{-1} of alkalinity at the river mouth could elevate the total carbon uptake in the Amazon River plume by 0.07–0.1 $MtCO_2$ month^{-1}. Such thought experiments are useful in designing minimalistic field trials and setting achievable goals for monitoring, reporting, and verification purposes.

1 Introduction

To meet the Paris Agreement goal of limiting global temperature change to well below 2°C (UNFCCC, 2015), reducing greenhouse gas emissions is urgently needed, but insufficient on its own. Modeling results from the IPCC (2022) estimate a total remaining carbon budget of less than 500 $GtCO_2$ for a >50% probability of staying below 1.5°C warming by 2100. Staying within this small remaining budget is a formidable challenge, as it requires current emissions rates, which totaled ~36 $GtCO_2$ yr^{-1} in 2021 (Friedlingstein et al., 2021), to rapidly approach zero. Accordingly, even very optimistic emission reduction scenarios assume carbon dioxide removal (CDR) will be needed to remove 10–20 $GtCO_2$ yr^{-1} from the atmosphere by the end of the century (NASEM, 2019; 2021). With the ocean covering ~70% of the Earth's surface and providing the largest sink for anthropogenic CO_2 emissions to date, there is growing interest in CDR solutions in the marine environment.

Several ocean-based CDR approaches have been suggested over the past decades to reduce CO_2 in the atmosphere (NASEM, 2021). Enhanced Weathering (EW) and Ocean Alkalinity Enhancement (OAE) are related techniques with the primary goal to accelerate the carbonate weathering process that would naturally remove atmospheric CO_2 at a very slow rate (10,000 to 100,000 years; Gonzalez and Ilyina, 2016). EW techniques involve pulverization of carbonate- rich rocks and their application on land, while OAE applies those materials to increase alkalinity at the ocean surface (Kheshgi, 1995; Bach et al., 2019). When carbonate materials are spread near the edge of a coastal watershed, the weathering process may happen on land and/or in the ocean, and the distinction between the two techniques blurs.

EW and OAE can have other co-benefits besides reducing CO_2 and mitigating global warming. Several early EW experiments via regional-scale liming focused on mitigating acidification in inland lakes and ambient streams. These studies found that the surface water pH could be elevated to desired levels and persist for years without causing deleterious effects to the environment (e.g., Wright, 1985; Porcella, 1989; Driscoll et al., 1996). EW deployments in agricultural settings have also been proven effective in

https://doi.org/10.5194/egusphere-2022-1505
Preprint. Discussion started: 5 January 2023

reducing soil acidity, preventing soil erosion, and enhancing crop yields (Caires et al., 2006; Köhler et al., 2010; Kantzas et al., 2022). Similarly, OAE can increase the pH of seawater, alleviating ocean acidification, which is a major stressor for the marine ecosystem (e.g., Doney et al., 2009). Both EW and OAE approaches are still in early phases of conceptualization and most OAE studies so far have focused on numerical simulations or efforts within laboratories (Köhler et al., 2010; Gonzalez and Ilyina, 2016; Moras et al., 2022; Wang et al., 2022). Understanding the feasibility, effectiveness, and ecological risks of OAE is required before any large-scale efforts should be implemented (NASEM, 2021). Though harmful ecosystem effects associated with highly elevated alkalinity cannot be ruled out (Bach et al., 2019), this risk must be weighed against a counterfactual in which carbon dioxide remains in the atmosphere.

Large river-dominated tropical oceans are potential test ground for OAE, for several reasons. First, mixing and subduction of surface waters into the ocean interior is minimized in tropical oceans relative to higher latitudes (Gonzalez and Ilyina, 2016; Lenton et al., 2018). Second, large rivers form surface plumes that extend thousands of kilometers offshore (Lentz and Limeburner, 1995; Coles et al., 2013). In combination, these two factors mean that added alkalinity would have a long time to absorb CO_2 at the surface ocean and impact a vast area along the plume path. During this time, the atmospheric CO_2 is continuously sequestered by the ocean until a new air-sea CO_2 equilibrium is reached. The plumes also have a heightened potential for observational tracking using surface salinity, which can be estimated from satellite observations. Finally, the carbonate-poor river waters may help suppress secondary chemical precipitation of the added alkalinity, a risk that can reduce the efficiency of OAE (Bach et al., 2019; Hartmann et al., 2022). Overall, global deployment of alkalinity in rivers is seen as CDR technique with the potential to scale to the gigaton level (Zhang et al., 2022).

Therefore, we examine the Amazon River-ocean continuum for its potential as a site of OAE. As the world's largest river by volume, the Amazon River represents ~20% of the global riverine discharge into the oceans (Salati and Vose, 1984). Its massive outflow (an average of ~0.2 Sverdrup; Figure S1) creates a thin surface layer of low-salinity (Figure 1) and low-carbonate plume, extending up to 1.5×10^6 km^2 at the ocean's surface (Molleri et al., 2010). As a result, the Amazon River plume has profound influence on the carbonate dynamics and atmospheric CO_2 sequestration throughout the western tropical North Atlantic Ocean (Ternon et al., 2000; Cooley et al., 2007; Lefèvre et al., 2010; Ibánez et al., 2015; Mu et al., 2021).

In this study of hypothetical alkalinity addition at the Amazon River mouth, we investigate the expected changes in air-sea CO_2 flux at the offshore Amazon plume waters and examine what the perturbation size and sampling density would be needed to measure the alkalinity change and verify a resultant anomalous CO_2 flux. We make use of the knowledge from previous field studies of the carbonate chemistry in the Amazon River plume, to address two main goals: 1) Analyze the potential for detectability of OAE-induced alkalinity change relative to measurement precision, background variability, and sample size; and 2) Estimate changes in ocean pCO_2 and air-sea CO_2 flux in the Amazon River plume due to hypothetical alkalinity addition at river mouth. Our effort aims to outline how one might consider the measurement, reporting and verification (MRV) needed in the context of known background variability. We argue that this kind of "thought experiment" is a first step that could lead to more realistic numerical simulations if the system does not fail basic tests of feasibility.

2 Method

2.1 Study Site and mixing model

We use a river-ocean conservative mixing model (Cooley and Yager, 2006) informed by direct observations collected as parts of the ANACONDAS and ROCA projects (Mu et al., 2021; Mu et al., in revision) to establish expectations of how alkalinity

https://doi.org/10.5194/egusphere-2022-1505
Preprint. Discussion started: 5 January 2023

perturbations would influence the carbonate system in the Amazon plume (the gray and green pathways on the methods schematic shown in Figure 2). The mixing model assumes no sources or sinks of the carbonate species modeled, and the deviations from this assumption are discussed in Section 2.2. In this model, dissolved inorganic carbon (DIC) and total alkalinity (TA) are treated as conservative tracers and used to describe pCO_2 variations as a function of salinity and temperature (Figure 1). TA and DIC can be respectively expressed as:

$$TA = [HCO_3^-] + 2[CO_3^{2-}] + \text{minor constituents} \quad (1)$$

$$DIC = [HCO_3^-] + [CO_3^{2-}] + [CO_2] \quad (2)$$

To establish the baseline condition of the carbonate system in the Amazon River-ocean continuum, we adopted the river endmembers from Mu et al. (in revision; also, Table 1) and ocean endmembers from Mu et al. (2021). The conservative mixing model can be further expressed as:

$$SSS_{mix} = S_r \times f_r + SSS_o \times f_o \quad (3)$$

$$f_r + f_o = 1 \quad (4)$$

SSS_{mix} is the salinity for a plume sample; S_r is the salinity of the river endmember ($S_r = 0$); and SSS_o is the surface salinity of the ocean endmember. In Equation (4), f_r and f_o are the proportions of river and ocean in the sample, both of which can be solved when SSS_{mix} is known. The theoretical TA and DIC in the plume, TA_{mix} and DIC_{mix} at any given SSS_{mix} are then calculated from the known endmember properties and proportions via:

$$TA_{mix} = TA_r \times f_r + TA_o \times f_o \quad (5)$$

$$DIC_{mix} = DIC_r \times f_r + DIC_o \times f_o \quad (6)$$

Eventually, pCO_2^{mix} and pH_{mix} at a given salinity and observed temperature are calculated with CO2SYS (Lewis et al., 1998) from inputs of TA_{mix} and DIC_{mix}. In this calculation we use the carbonic acid dissociation constants K1 and K2 from Mehrback (1973), refit by Dickson and Millero (1987).

We confined our study periods to two specific months, September 2011 and July 2012, during which measurements were made in both the river and throughout the Amazon River plume. Details in quantifying the river endmembers are described in Ward et al. (2015) and Mu et al. (in revision). Briefly, six river samples were collected at each gateway near the Amazon River mouth in each month and analyzed for TA and DIC. For a concise demonstration, we use one single outer gateway, North Macapá, to represent the Amazon River mouth in this study, while using the means and standard deviations of the six TA values as the river TA endmembers and their natural variability, respectively (Table 1). The monthly CO_2 fluxes in the plume for both chosen months are displayed in Table 2.

2.2 Deviations from the conservative mixing model

The assumption that TA and DIC act as conservative tracers is not true in the presence of photosynthesis, respiration, calcification, and/or air-sea gas exchange. In fact, plume pCO_2 values measured from an underway system on the research vessels surveying for the ANACONDAS program were systematically lower than predicted from the mixing model (Mu et al., 2021). This offset was assumed to be due to net community production, an assumption supported by the strong correlation between shipboard chlorophyll and the difference between the pCO_2^{mix} calculated from conservative mixing and the measured pCO_2 (Mu et al., 2021).

https://doi.org/10.5194/egusphere-2022-1505
Preprint. Discussion started: 5 January 2023

A linear regression between measured SSS (15 < SSS < 35) and measured pCO_2 showed a strong linear relationship (r = 0.79 for September 2011 and r = 0.97 for July 2012). Therefore, we use SSS to calculate an empirical estimate of pCO_2 ($pCO_2^{empirical}$) at every SSS level in each month (orange pathway in the schematic shown as Figure 2). SSS fields in the Amazon plume were derived from remotely sensed diffuse attenuation coefficient at 490 nm (K_d490, Figure 1). The measured-SSS vs $pCO_2^{empirical}$ regression is used to map $pCO_2^{empirical}$ at every satellite-derived SSS value in the plume (as in Figure 3a) and to calculate the empirical air-sea CO_2 flux, according to the following equation:

$$Flux_{empirical} = k\alpha(pCO_2^{empirical} - pCO_2^{atm}) \qquad (7)$$

Where k is the gas exchange coefficient calculated from gridded reanalysis wind speed and the parameterization of Sweeney et al. (2007), α is the solubility of CO_2 in seawater, and pCO_2^{atm} is the monthly averaged pCO_2 in the atmosphere measured at a nearby NOAA monitoring station. Details in calculating the empirical CO_2 flux can be found in Mu et al. (2021).

2.3 Experimental Design

The core of our thought experiment is to manipulate the concentrations of TA at the river mouth by the hypothetical addition of pulverized quicklime (CaO), assuming the additional CaO converts 100% to TA according to stoichiometry. The dissolution of CaO consumes CO_2 and releases HCO_3^- through:

$$(CaO + H_2O \rightleftharpoons Ca(OH)_2) + 2\,CO_2 \rightleftharpoons Ca^{2+} + 2\,HCO_3^- \qquad (8)$$

For every mole of additional CaO, TA is increased by 2 moles while DIC remains constant (i.e., consuming 2 moles of CO_2 while producing 2 moles of bicarbonate) before any significant air-sea equilibration occurs. Because CaO dissolution happens on hour-scales (Moras et al., 2022) while the air-sea CO_2 equilibration usually takes weeks in the western tropical North Atlantic (Jones et al., 2014), the assumption of a constant DIC perturbation should hold over the time scale of dissolution. We assume in this study that there is no secondary precipitation of $CaCO_3$, and that the additional CaO stays at the surface layer until fully dissolved. We will address key unknowns associated with these assumptions in the discussion.

We explore TA perturbations over the range 1–100 μmol kg^{-1} (i.e., perturbation between 0.07 and 7 times the natural variability for September 2011 and 0.04 and 4 times the natural variability for July 2012). The mixing model is recalculated with each of the perturbed river endmembers to find the perturbed TA_{mix} and DIC_{mix} across the plume. Then we use CO2SYS to calculate the theoretical $pCO_2^{mix\_OAE}$ at each salinity stamp with the perturbed TA_{mix}, DIC_{mix} and observed temperature as inputs to compare to the unperturbed baseline. The difference of the TA-enhanced seawater pCO_2 and the baseline pCO_2:

$$\Delta_{OAE}pCO_2^{mix} = pCO_2^{mix\_OAE} - pCO_2^{mix\_base} \qquad (9)$$

In each perturbation scenario, the added alkalinity lowers the $pCO_2^{mix\_OAE}$ below the unperturbed mixing curve by the amount of $\Delta_{OAE}pCO_2^{mix}$. To finally arrive at the surface ocean pCO_2 needed to calculate the air-sea fluxes according to Equation 7, we add the $\Delta_{OAE}pCO_2^{mix}$ to $pCO_2^{empirical}$:

$$pCO_2^{OAE} = \Delta_{OAE}pCO_2^{mix} + pCO_2^{empirical} \qquad (10)$$

This approach (schematized in Figure 2) implicitly assumes that the biological processes that lower the measured $pCO_2^{empirical}$ below the theoretical pCO_2^{mix} would be unchanged from the deployment of additional alkalinity, an assumption that would demand careful testing in the field.

https://doi.org/10.5194/egusphere-2022-1505
Preprint. Discussion started: 5 January 2023

2.4 Sensitivity analysis for detectability of hypothetical OAE deployments

We use a simple bootstrapping technique (or Monte Carlo simulation) to assess the minimum TA perturbation that would be detectable with a given number of measurements, taking into consideration the background variability during a given season and reasonable measurement precision.

We randomly generate 10,000 baseline TA values under a normal distribution using the mean and standard deviation of the six measured TA values in September 2011 or July 2012. We then generate 10,000 perturbed TA values for each perturbation scenario under a normal distribution, where the mean is the addition of the baseline mean and the perturbation strength, with the same standard deviation as the baseline. The range for the tested perturbation sizes is 1–20 μmol kg^{-1} of TA. Within the 10,000 TA pools from both the baseline and a perturbation scenario, we randomly select 1–100 values (i.e., varying sample size) from both pools, perform the Student's t-test between the selected sets, and calculate the p-value to determine if the perturbed TA set would be seen as significantly different from baseline. The t-test is repeated 1,000 times for each perturbation size and sample size, generating 1,000 p-values. The mean of those p-values are calculated for each perturbation scenario at each sample size (Figure 4). A lower p-value suggests higher likelihood that the perturbed TA values would be considered significantly different from the baseline, and therefore "detectable". We use a threshold of $p < 0.1$ to indicate statistical significance.

3 Results

3.1 Baseline carbon chemistry in the plume

The surface $pCO_2^{empirical}$ in the Amazon River plume derived from remotely sensed SSS generally ranged from 210–400 μatm in September 2011 (Figure 3a), with lowest values in low-salinity regions near French Guiana coast and increasing as the river mixes with ocean water (Figure 1a). Figure 3a masks out regions with surface salinity below 15 and beyond 35 psu, as these waters are out of the range of a sufficiently robust algorithm between K_d490 and SSS (Mu et al., 2021).

The distribution of plume surface pCO_2^{sw} is primarily shaped by two processes: the Amazon River-ocean mixing and biological CO_2 consumption/release in the plume waters (Mu et al., 2021). For example, zero-salinity river water near the mouth is supersaturated with respect to atmospheric CO_2 in July 2012, where pCO_2 >1,000 μatm is observed (Mu et al., 2021; Mu et al., in revision) due to low carbonate buffer capacity and high microbial respiration. As the river waters mix with the ocean, the sharp increase in buffer capacity and shift towards a net autotrophic state lower the surface pCO_2 towards a minimum (below pCO_2^{atm} in July 2012; Mu et al., 2021) before rising towards the open ocean levels closer to equilibrium with the atmosphere (i.e., pCO_2 ~400 μatm) at higher salinity. The nitrogen-fixing diatom-diazotroph assemblages and other phytoplankton that are active in the Amazon plume waters (Goes et al., 2014) further enhance the CO_2 undersaturation in mid- to mid-high salinity portions of the plume (i.e., $15 < SSS < 33$) on top of the undersaturated CO_2 state caused by conservative mixing (Mu et al., 2021).

3.2 Detectability of TA perturbations

We propose that the minimum requirement for MRV in a watershed OAE experiment is that the perturbed TA in the river can be detected above background variability. To illustrate the challenge of detectability, we consider the background TA variability in the North Macapá gateway in September 2011, with the assumption that the variability measured at that time (standard deviation 14.5 μmol kg^{-1}) is representative of that season and gateway. It is intuitive that a large enough perturbation (commensurate with the standard deviation) is detectable with a small number of samples (Figure 4), and a small perturbation (a factor of 3 smaller than the standard deviation or smaller) cannot be detected against the background variability regardless of the number of samples. This

https://doi.org/10.5194/egusphere-2022-1505
Preprint. Discussion started: 5 January 2023

exercise reveals the challenge of balancing the effort needed to detect the perturbation against the obstacle and risk of increasing the TA by a large amount.

As expected and illustrated in Figure 4, higher sample sizes and TA perturbations lead to greater detectability of the alkalinity enhancement. For practical purposes, neither sample size nor perturbation strength can be increased infinitely, so OAE experiments would likely seek a balance between the two. For example, in September 2011 (Figure 4a, c), a TA perturbation of ~7–10 μmol kg^{-1} would have been readily detectable with 40 samples. For July 2012 (Figure 4b, d), when background variability was higher (25.7 μmol kg^{-1}), 40 samples would detect perturbations only if they were to exceed +20 μmol kg^{-1} of TA. Each gateway and season may have different background variability that would require measurement and characterization in advance of any perturbation to have a clear strategy for sampling.

3.3 Impact on pCO_2 and air-sea CO_2 flux

Figure 3b shows the pCO_2^{mix} decrease due to a hypothetical TA addition in the Amazon watershed, which is highest in the low-salinity waters near the river mouth and attenuates at higher salinities due to mixing with the unperturbed ocean water. Figure 5 provides a quantification of the air-sea CO_2 flux at each salinity level for different TA perturbation strengths (20, 50 and 100 μmol kg^{-1}). While the air-sea CO_2 flux per unit area (or flux density) is greatest at low salinities (Figure 5a, b), the large area occupied by the diluted plume (salinities greater than 25) means that more than half of the total integrated air-sea CO_2 exchange – as well as the perturbation to this flux – would occur in this salty part of the plume.

Air-sea CO_2 exchange at SSS = 34–35 for July 2012 is only slightly greater than 0 (Figure 5b), but due to the large area of plume at near-oceanic salinity level, the total plume CO_2 uptake (i.e., negative flux) in lower S regions is entirely offset by the CO_2 outgassing at 34 < SSS < 35. Regardless of whether the baseline Amazon plume is a carbon sink or source, the change in air-sea CO_2 exchange due to OAE shifts toward more carbon storage by the ocean and increases linearly with the size of TA perturbation (Table 2).

4 Discussion

4.1 Exploring the minimum TA detectability

Here we propose that the minimum MRV requirement for an OAE experiment in a river be that the TA increase can be detected in the fresh river endmember, and we showed what size perturbation and sampling density would meet that minimum for the Amazon River. We found that the minimum detectable TA addition at the Amazon River mouth ranges between 10–20 μmol kg^{-1} with a reasonable sample size of 40 during field campaigns before and during the perturbation (Figure 4c, d).

One may further hope that MRV efforts for OAE deployed at the river mouth would document reductions in plume pCO_2. We rely on the observed pCO_2, a mixing model, and satellite-derived SSS to deduce where one might expect pCO_2 reductions to be measurable relative to background concentrations. Sensors for measuring pCO_2^{sw} aboard ships and uncrewed surface vehicles like Saildrone and Waveglider have a target accuracy of 2 μatm (Sabine et al., 2020). Figure 3 shows that, if Amazon River water TA were continuously increased by 20 μmol kg^{-1}, a broad region of the plume would see pCO_2^{sw} decreases measurable with current sensor technology, if they could sustain regular sampling over the SSS < 30 region before, during, and after the OAE deployment.

However, like with the detectability of the TA in the river mouth, the pCO_2 perturbation must be detectable given background variability, and does not depend only on sensor accuracy. Here, a measure of that background variability is the RMS error between the $pCO_2^{empirical}$, calculated from the linear regression of the *in situ* observations of pCO_2 and SSS, and the actual observations of

https://doi.org/10.5194/egusphere-2022-1505
Preprint. Discussion started: 5 January 2023

pCO_2 (Figure 2). For September 2011, the RMS error of this regression is ~22 μatm (data not shown). Thus, we would expect that a perturbation approximately this size would be detectable with sufficient samples. Figure 3 suggests that a region of the plume near the river mouth could meet this criterion, given a TA perturbation of +20 μmol kg^{-1} in the river.

It is encouraging that SSS can be estimated from satellite measurements, allowing for field campaigns – including uncrewed vehicles piloted from operators onshore – to find and sample in the plume where an OAE-induced pCO_2 reduction may be detected. Nevertheless, Figure 5 shows that nearly half the additional ocean CO_2 uptake due to the OAE experiment could happen in the part of the plume with $30 < SSS < 35$, where detecting the perturbation in TA and plume surface pCO_2 is impossible with the accuracy of existing sensors or the laboratory analysis of bottle measurements.

Finally, we consider the amount of limestone ($CaCO_3$) required to produce pulverized quicklime as the alkalinity source material that sustains a set TA perturbation size (Table 2). The limestone equivalents needed to create a detectable perturbation of +20 μmol kg^{-1} of TA is 0.4 Mt per month using river discharge numbers from September 2011, which is approximately equal to 0.04% of US industrial limestone production in the year 2021 (USGS, https://pubs.usgs.gov/periodicals/mcs2021/mcs2021-stone-crushed.pdf). Using river discharge for July 2012, the requirement grows to 0.7 Mt limestone per month. In terms of OAE-induced additional CO_2 uptake, every 0.1 $MtCO_2$ month^{-1} represents more than 30 times greater CDR than the CO_2 captured by one ORCA Direct Air Capture plant in a full year (https://en.wikipedia.org/wiki/Orca_(carbon_capture_plant)), yet amounts to less than what Brazil emitted on an average 2 hour basis in 2021 (https://www.icos-cp.eu/science-and-impact/global-carbon-budget/2021). It is worth noting that concerns have been raised over the feasibility of CaO liming considering the energy need and CO_2 release associated with the production of this alkalinity source (e.g., Renforth et al., 2013; Voosen, 2022), but limestone calcination coupled with heat recovery and carbon capture & storage technologies is found to significantly reduce energy costs and CO_2 emission during CaO production, potentially making this liming approach more sustainable (Foteinis et al., 2022).

4.2 Constraints on OAE deployments

So far, we have focused most of our efforts on describing the minimum detectable OAE perturbation. It is also important to consider what might constrain the upper limit of TA addition (i.e., through liming), such as ecosystem disturbances and secondary precipitation of calcium carbonate. Ideally, OAE would not put the ambient marine ecosystems at risk. The minimum detectable perturbation described above is so close to the background TA variability that we suspect it would have negligible impact on the ecosystem. Heavy metals in some source alkaline minerals are problematic (NASEM, 2021), a consideration avoided with the use of 100% pure CaO compound as the source of TA addition. The highest perturbation we explored was +100 μmol kg^{-1} of TA added to the river endmember, which would lead to initial pH increase of 2.0 at the river mouth, a pCO_2^{sw} decrease of up to 100 μatm (data not shown) in the Amazon plume, and a total enhanced atmospheric carbon uptake of ~0.35 $MtCO_2$ month^{-1} across the plume during September 2011 (Table 2 and Figure 5c). While the level of initial pH increase at the TA addition site may be concerning for local marine communities, the effect would be quickly dispersed by the river, and is reduced with increasing distance from the river due to mixing with the ocean.

Another constraint on the upper limit of TA addition through ocean liming is secondary $CaCO_3$ precipitation and the resulting reduction of atmospheric CO_2 uptake. Moras et al. (2022) suggested that runaway $CaCO_3$ during OAE may be avoidable if the saturation state of aragonite (Ω_A) is kept below 5 for natural seawater. Assuming such a Ω_A threshold for barely avoiding $CaCO_3$ precipitation is also applicable in fresher Amazon plume and river water, we have calculated the corresponding maximum TA perturbation allowed to keep Ω_A below this threshold according to the method in Mucci (1983), with the results shown in Table 3. Because the Ω_A increases with salinity, TA perturbation that likely avoids secondary $CaCO_3$ precipitation becomes substantially

https://doi.org/10.5194/egusphere-2022-1505
Preprint. Discussion started: 5 January 2023

smaller close to S=35 (i.e., ~100 μmol kg^{-1}, compared to ~260 μmol kg^{-1} at S=0). Adding 20 μmol kg^{-1} of TA in September 2011 would only increase Ω_A by a maximum of 0.3 (Table 3), and Ω_A stays below 5 everywhere in the plume for TA additions of 100 μmol kg^{-1} or smaller. An important caveat on assuming a Ω_A threshold of 5 is that the Amazon River at the mouth contains heavy loads of mineral particles and will likely facilitate the formation of heterogenous nucleation and precipitation for $CaCO_3$ (Renforth and Henderson, 2017; Moras et al., 2022), thereby lowering the maximum TA addition allowed. Further study is needed to ensure Ω_A is always kept below proper precipitation threshold in all regions of the river plume.

Adding TA to the land surrounding the Amazon watershed has possible advantages over spreading over the open ocean, involving co-benefits to the terrestrial ecosystems and agriculture, such as increased crop yield in agricultural watersheds (Caires et al., 2006; Hartmann et al., 2013; Beerling et al., 2020; Kelland et al., 2020), reduced soil run-off (Taylor et al., 2016), and reduction of N_2O production (Beerling et al., 2018). Introducing the lime on land might also slow its dissolution in the river, helping reduce the risks associated with large perturbations to pH and TA, like secondary precipitation or phytoplankton community perturbations. However, deployment on land would likely increase the difficulty to quantify the effect of TA addition for MRV purposes.

4.3 Additional challenges

One of the underlying assumptions for this analysis is that CaO reacting with CO_2 takes place in a time frame faster than air-sea re-equilibration to occur, and the layer of plume water dwells at the surface for a relatively long period of time. If the TA-enhanced surface plume is not exposed to the atmosphere long enough to allow for full air–sea CO_2 equilibration (e.g., due to water mass subduction), CO_2 removal efficiency will decrease in these regions (Jones et al., 2014). A logical next step to characterize the spatial footprint of the hypothetical experiment and the total time scale for equilibration would be to simulate the time-evolving patch of the alkalinity anomaly, the corresponding pCO_2 perturbation, and the total excess DIC in an ocean general circulation model with the OAE experiment relative to a control simulation.

We argue that the TA-enhanced waters do not need to remain continuously within the surface layer to induce ocean CDR. The change in the air-sea flux can be realized whenever the perturbed waters influence the surface, even if that is far from the plume or years after the deployment. Though the implied dilution of the signal or delay in causing additionality of the CDR may not change the net impact of the OAE experiment if integrated over a sufficiently long time period, it would make MRV of the total impact essentially impossible through observational methods alone.

Another assumption in this work was that the photosynthesis, which is known to drive pCO_2 beneath the conservative mixing curve (Mu et al., 2021), would be unchanged by the alkalinity addition. This assumption is premised on the argument that perturbations barely detectable above background variability are unlikely to strongly change the ambient ecosystem. Regardless, ecosystem impacts would require careful monitoring in any field experiment. Recent results from a mesocosm experiment with Tasmanian coastal waters show statistically significant, though relatively moderate, changes to phytoplankton community structure and function at high TA perturbation values of +495 μmol kg^{-1}, which is 25 times higher than the minimum detectable perturbation explored here (Ferderer et al., 2022).

If the alkalinity source for OAE is quicklime, managing the heat released through its exothermic reaction during dissolution in water at a rate of 64 kJ mol^{-1} CaO is another important consideration. Taking the highest perturbation scenario explored in Table 2 that increases TA in the Amazon watershed by 100 μmol kg^{-1}, we estimate 310 MW total heat released during the duration of the dissolution. In order for the heat released from the CaO reaction to be lower than 10% of the daily solar radiation at the equator ~400 W m^{-2} (a level that would presumably be swamped by natural variability in the river's heat budget), the TA injection would have to occur over an area of river larger than about 8 km^2, e.g., 2 km of river width and 4 km along its length. Therefore, it is

https://doi.org/10.5194/egusphere-2022-1505
Preprint. Discussion started: 5 January 2023

possible to minimize the environmental risk due to heat released during quicklime dissolution by spreading it over a large enough area at the river mouth.

5 Conclusions

We propose a thought experiment of alkalinity enhancement in the Amazon River watershed, evaluating the detectability of added TA, and predicting its influence on the atmospheric CO_2 uptake in the offshore plume. Adding 20 μmol kg^{-1} of TA in a month at the Amazon watershed could increase the CO_2 uptake by the river plume by 0.07–0.1 MtCO$_2$ month^{-1}. We found a TA perturbation of +10–20 μmol kg^{-1} in the river is readily detectable with at least 40 samples, given background variability of 15–30 μmol kg^{-1}. By adding a TA perturbation barely detectable relative to the background TA variability, the likelihood of substantial environmental disturbance at the injection site would be minimized. However, observing the corresponding pCO_2 perturbation in the plume presents a greater observational challenge. Even with the highly sensitive pCO_2 sensors available today (e.g., Sabine et al., 2020), detectability of the pCO_2 anomaly is plausible only in the freshest part of the plume given dilution of the signal at higher salinities and large background variability. Finally, quantifying the total additional CO_2 uptake from this type of OAE cannot rely on observations alone; idealized conceptual models like the one presented here and more sophisticated circulation-biogeochemical ocean models will always be required to understand the total CDR because the additional CO_2 uptake is likely to occur over long time periods and at very diluted perturbation levels.

Data availability

Data for the air–sea CO_2 flux calculations in the Amazon River plume are from Mu et al. (2021). River mouth data are reported in a manuscript currently under revision in *Global Biogeochemical Cycles* that will be resubmitted in January 2023. All codes are available at https://drive.google.com/drive/folders/1YYjcT5ZYvyHoJaKmRl3Fd8aagMhtRwCA?usp=share_link.

Author Contribution

JBP and LM conceptualized the framework of this experiment. LM, JBP, and HW designed the methodology. LM performed the analytical calculations and numerical simulations. LM wrote the manuscript with support from JBP and HW. JBP supervised the project.

Competing Interests

The authors declare that they have no conflict of interest.

Acknowledgement

We would like to thank Patricia Yager for leading the ANACONDAS and ROCA projects that lay the foundation of this manuscript. LM thanks Jessica Cross, Brendan Carter, Charly Moras, Sijia Dong, and Bo Yang for contributing to discussions, and Sarah Nickford for assistance with figure production.

https://doi.org/10.5194/egusphere-2022-1505
Preprint. Discussion started: 5 January 2023

Reference

Bach, L. T., Gill, S. J., Rickaby, R. E. M., Gore, S., and Renforth, P.: CO2 Removal With Enhanced Weathering and Ocean Alkalinity Enhancement: Potential Risks and Co-benefits for Marine Pelagic Ecosystems, Frontiers in Climate, 1, 2019.

Beerling, D. J., Leake, J. R., Long, S. P., Scholes, J. D., Ton, J., Nelson, P. N., Bird, M., Kantzas, E., Taylor, L. L., Sarkar, B., Kelland, M., DeLucia, E., Kantola, I., Müller, C., Rau, G., and Hansen, J.: Farming with crops and rocks to address global climate, food and soil security, Nature Plants, 4, 138–147, https://doi.org/10.1038/s41477-018-0108-y, 2018.

Beerling, D. J., Kantzas, E. P., Lomas, M. R., Wade, P., Eufrasio, R. M., Renforth, P., Sarkar, B., Andrews, M. G., James, R. H., Pearce, C. R., Mercure, J.-F., Pollitt, H., Holden, P. B., Edwards, N. R., Khanna, M., Koh, L., Quegan, S., Pidgeon, N. F., Janssens, I. A., Hansen, J., and Banwart, S. A.: Potential for large-scale CO2 removal via enhanced rock weathering with croplands, Nature, 583, 242–248, https://doi.org/10.1038/s41586-020-2448-9, 2020.

Caires, E. F., Barth, G., and Garbuio, F. J.: Lime application in the establishment of a no-till system for grain crop production in Southern Brazil, Soil and Tillage Research, 89, 3–12, https://doi.org/10.1016/j.still.2005.06.006, 2006.

Coles, V. J., Brooks, M. T., Hopkins, J., Stukel, M. R., Yager, P. L., and Hood, R. R.: The pathways and properties of the Amazon River Plume in the tropical North Atlantic Ocean, Journal of Geophysical Research: Oceans, 118, 6894–6913, https://doi.org/10.1002/2013JC008981, 2013.

Cooley, S. R. and Yager, P. L.: Physical and biological contributions to the western tropical North Atlantic Ocean carbon sink formed by the Amazon River plume, Journal of Geophysical Research: Oceans, 111, https://doi.org/10.1029/2005JC002954, 2006.

Cooley, S. R., Coles, V. J., Subramaniam, A., and Yager, P. L.: Seasonal variations in the Amazon plume-related atmospheric carbon sink, Global Biogeochemical Cycles, 21, https://doi.org/10.1029/2006GB002831, 2007.

Dickson, A. G. and Millero, F. J.: A comparison of the equilibrium constants for the dissociation of carbonic acid in seawater media, Deep Sea Research Part A. Oceanographic Research Papers, 34, 1733–1743, https://doi.org/10.1016/0198-0149(87)90021-5, 1987.

Doney, S. C., Fabry, V. J., Feely, R. A., and Kleypas, J. A.: Ocean Acidification: The Other CO2 Problem, Annual Review of Marine Science, 1, 169–192, https://doi.org/10.1146/annurev.marine.010908.163834, 2009.

Driscoll, C. T., Cirmo, C. P., Fahey, T. J., Blette, V. L., Bukaveckas, P. A., Burns, D. A., Gubala, C. P., Leopold, D. J., Newton, R. M., Raynal, D. J., Schofield, C. L., Yavitt, J. B., and Porcella, D. B.: The experimental watershed liming study: Comparison of lake and watershed neutralization strategies, Biogeochemistry, 32, 143–174, https://doi.org/10.1007/BF02187137, 1996.

Ferderer, A., Chase, Z., Kennedy, F., Schulz, K. G., and Bach, L. T.: Assessing the influence of ocean alkalinity enhancement on a coastal phytoplankton community, Biogeosciences, 19, 5375–5399, https://doi.org/10.5194/bg-19-5375-2022, 2022.

Foteinis, S., Andresen, J., Campo, F., Caserini, S., and Renforth, P.: Life cycle assessment of ocean liming for carbon dioxide removal from the atmosphere, J. Clean. Prod., 370, 133309, https://doi.org/10.1016/j.jclepro.2022.133309, 2022.

Friedlingstein, P., Jones, M. W., O'Sullivan, M., Andrew, R. M., Bakker, D. C. E., Hauck, J., Le Quéré, C., Peters, G. P., Peters, W., Pongratz, J., Sitch, S., Canadell, J. G., Ciais, P., Jackson, R. B., Alin, S. R., Anthoni, P., Bates, N. R., Becker, M., Bellouin, N., Bopp, L., Chau, T. T. T., Chevallier, F., Chini, L. P., Cronin, M., Currie, K. I., Decharme, B., Djeutchouang, L. M., Dou, X., Evans, W., Feely, R. A., Feng, L., Gasser, T., Gilfillan, D., Gkritzalis, T., Grassi, G., Gregor, L., Gruber, N., Gürses, Ö., Harris, I., Houghton, R. A., Hurtt, G. C., Iida, Y., Ilyina, T., Luijkx, I. T., Jain, A., Jones, S. D., Kato, E., Kennedy, D., Klein Goldewijk, K., Knauer, J., Korsbakken, J. I., Körtzinger, A., Landschützer, P., Lauvset, S. K., Lefèvre, N., Lienert, S., Liu, J., Marland, G., McGuire, P. C., Melton, J. R., Munro, D. R., Nabel, J. E. M. S., Nakaoka, S.-I., Niwa, Y., Ono, T., Pierrot, D., Poulter, B., Rehder, G., Resplandy, L., Robertson, E., Rödenbeck, C., Rosan, T. M., Schwinger, J., Schwingshackl, C., Séférian, R., Sutton, A. J., Sweeney, C., Tanhua, T., Tans, P. P., Tian, H., Tilbrook, B., Tubiello, F., van der Werf, G. R., Vuichard, N., Wada, C., Wanninkhof, R., Watson, A. J., Willis, D., Wiltshire, A. J., Yuan, W., Yue, C., Yue, X., Zaehle, S., and Zeng, J.: Global Carbon Budget 2021, Earth System Science Data, 14, 1917–2005, https://doi.org/10.5194/essd-14-1917-2022, 2022.

Goes, J. I., Gomes, H. do R., Chekalyuk, A. M., Carpenter, E. J., Montoya, J. P., Coles, V. J., Yager, P. L., Berelson, W. M., Capone, D. G., Foster, R. A., Steinberg, D. K., Subramaniam, A., and Hafez, M. A.: Influence of the Amazon River discharge on the biogeography of phytoplankton communities in the western tropical north Atlantic, Progress in Oceanography, 120, 29–40, https://doi.org/10.1016/j.pocean.2013.07.010, 2014.

González, M. F. and Ilyina, T.: Impacts of artificial ocean alkalinization on the carbon cycle and climate in Earth system simulations, Geophysical Research Letters, 43, 6493–6502, https://doi.org/10.1002/2016GL068576, 2016.

https://doi.org/10.5194/egusphere-2022-1505
Preprint. Discussion started: 5 January 2023

Hartmann, J., West, A. J., Renforth, P., Köhler, P., De La Rocha, C. L., Wolf-Gladrow, D. A., Dürr, H. H., and Scheffran, J.: Enhanced chemical weathering as a geoengineering strategy to reduce atmospheric carbon dioxide, supply nutrients, and mitigate ocean acidification, Reviews of Geophysics, 51, 113–149, https://doi.org/10.1002/rog.20004, 2013.

Hartmann, J., Suitner, N., Lim, C., Schneider, J., Marín-Samper, L., Arístegui, J., Renforth, P., Taucher, J., and Riebesell, U.: Stability of alkalinity in Ocean Alkalinity Enhancement (OAE) approaches – consequences for durability of CO_2 storage, Biogeosciences Discussions, 1–29, https://doi.org/10.5194/bg-2022-126, 2022.

Ibánhez, J. S. P., Diverrès, D., Araujo, M., and Lefèvre, N.: Seasonal and interannual variability of sea-air CO2 fluxes in the tropical Atlantic affected by the Amazon River plume, Global Biogeochemical Cycles, 29, 1640–1655, https://doi.org/10.1002/2015GB005110, 2015.

IPCC: Summary for Policymakers. In: Climate Change 2022: Impacts, Adaptation, and Vulnerability. Cambridge University Press, 2022.

Jones, D. C., Ito, T., Takano, Y., and Hsu, W.-C.: Spatial and seasonal variability of the air-sea equilibration timescale of carbon dioxide, Global Biogeochemical Cycles, 28, 1163–1178, https://doi.org/10.1002/2014GB004813, 2014.

Kantzas, E. P., Val Martin, M., Lomas, M. R., Eufrasio, R. M., Renforth, P., Lewis, A. L., Taylor, L. L., Mecure, J.-F., Pollitt, H., Vercoulen, P. V., Vakilifard, N., Holden, P. B., Edwards, N. R., Koh, L., Pidgeon, N. F., Banwart, S. A., and Beerling, D. J.: Substantial carbon drawdown potential from enhanced rock weathering in the United Kingdom, Nat. Geosci., 15, 382–389, https://doi.org/10.1038/s41561-022-00925-2, 2022.

Kheshgi, H. S.: Sequestering atmospheric carbon dioxide by increasing ocean alkalinity, Energy, 20, 915–922, https://doi.org/10.1016/0360-5442(95)00035-F, 1995.

Köhler, P., Hartmann, J., and Wolf-Gladrow, D. A.: Geoengineering potential of artificially enhanced silicate weathering of olivine, Proceedings of the National Academy of Sciences, 107, 20228–20233, https://doi.org/10.1073/pnas.1000545107, 2010.

Lefèvre, N., Diverrès, D., and Gallois, F.: Origin of CO_2 undersaturation in the western tropical Atlantic, Tellus B: Chemical and Physical Meteorology, 62, 595–607, https://doi.org/10.1111/j.1600-0889.2010.00475.x, 2010.

Lenton, A., Matear, R. J., Keller, D. P., Scott, V., and Vaughan, N. E.: Assessing carbon dioxide removal through global and regional ocean alkalinization under high and low emission pathways, Earth System Dynamics, 9, 339–357, https://doi.org/10.5194/esd-9-339-2018, 2018.

Lentz, S. J. and Limeburner, R.: The Amazon River Plume during AMASSEDS: Spatial characteristics and salinity variability, Journal of Geophysical Research: Oceans, 100, 2355–2375, https://doi.org/10.1029/94JC01411, 1995.

Lewis, E., Wallace, D., and Allison, L. J.: Program developed for CO{sub 2} system calculations, Brookhaven National Lab., Dept. of Applied Science, Upton, NY (United States); Oak Ridge National Lab., Carbon Dioxide Information Analysis Center, TN (United States), https://doi.org/10.2172/639712, 1998.

Mehrbach, C., Culberson, C. H., Hawley, J. E., and Pytkowicx, R. M.: Measurement of the Apparent Dissociation Constants of Carbonic Acid in Seawater at Atmospheric Pressure1, Limnology and Oceanography, 18, 897–907, https://doi.org/10.4319/lo.1973.18.6.0897, 1973.

Molleri, G. S. F., Novo, E. M. L. de M., and Kampel, M.: Space-time variability of the Amazon River plume based on satellite ocean color, Continental Shelf Research, 30, 342–352, https://doi.org/10.1016/j.csr.2009.11.015, 2010.

Moras, C. A., Bach, L. T., Cyronak, T., Joannes-Boyau, R., and Schulz, K. G.: Ocean alkalinity enhancement – avoiding runaway $CaCO_3$ precipitation during quick and hydrated lime dissolution, Biogeosciences, 19, 3537–3557, https://doi.org/10.5194/bg-19-3537-2022, 2022.

Mu, L., Gomes, H. do R., Burns, S. M., Goes, J. I., Coles, V. J., Rezende, C. E., Thompson, F. L., Moura, R. L., Page, B., and Yager, P. L.: Temporal Variability of Air-Sea CO2 flux in the Western Tropical North Atlantic Influenced by the Amazon River Plume, Global Biogeochemical Cycles, 35, e2020GB006798, https://doi.org/10.1029/2020GB006798, 2021.

Mu, L., Richey, J. E., Ward, N. D., Krusche, A. V., Montebelo, A, Rezende, C. E., Medeiros, P. M., Page, B. P., and Yager, P. L.: Carbonate and nutrient contributions from the Amazon River to the western tropical North Atlantic Ocean, Global Biogeochemical Cycles. In revision, 2022.

Mucci, A.: The solubility of calcite and aragonite in seawater at various salinities, temperatures, and one atmosphere total pressure, American Journal of Science, 283, 780–799, https://doi.org/10.2475/ajs.283.7.780, 1983.

National Academies of Sciences, Engineering, and Medicine: Negative emissions technologies and reliable sequestration: A research agenda, 2019.

https://doi.org/10.5194/egusphere-2022-1505
Preprint. Discussion started: 5 January 2023

National Academies of Sciences, Engineering, and Medicine: A research strategy for ocean-based carbon dioxide removal and sequestration, 2021.

Porcella, D. B.: Lake Acidification Mitigation Project (LAMP): an Overview of an Ecosystem Perturbation Experiment, Can. J. Fish. Aquat. Sci., 46, 246–248, https://doi.org/10.1139/f89-034, 1989.

Sabine, C., Sutton, A., McCabe, K., Lawrence-Slavas, N., Alin, S., Feely, R., Jenkins, R., Maenner, S., Meinig, C., Thomas, J., Ooijen, E. van, Passmore, A., and Tilbrook, B.: Evaluation of a New Carbon Dioxide System for Autonomous Surface Vehicles, Journal of Atmospheric and Oceanic Technology, 37, 1305–1317, https://doi.org/10.1175/JTECH-D-20-0010.1, 2020.

Salati, E. and Vose, P. B.: Amazon Basin: A System in Equilibrium, Science, 225, 129–138, https://doi.org/10.1126/science.225.4658.129, 1984.

Sweeney, C., Gloor, E., Jacobson, A. R., Key, R. M., McKinley, G., Sarmiento, J. L., and Wanninkhof, R.: Constraining global air-sea gas exchange for CO2 with recent bomb 14C measurements, Global Biogeochemical Cycles, 21, https://doi.org/10.1029/2006GB002784, 2007.

Taylor, L. L., Quirk, J., Thorley, R. M. S., Kharecha, P. A., Hansen, J., Ridgwell, A., Lomas, M. R., Banwart, S. A., and Beerling, D. J.: Enhanced weathering strategies for stabilizing climate and averting ocean acidification, Nature Clim Change, 6, 402–406, https://doi.org/10.1038/nclimate2882, 2016.

Ternon, J. F., Oudot, C., Dessier, A., and Diverres, D.: A seasonal tropical sink for atmospheric CO2 in the Atlantic ocean: the role of the Amazon River discharge, Marine Chemistry, 68, 183–201, https://doi.org/10.1016/S0304-4203(99)00077-8, 2000.

USGS, Crushed Stone Statistics and Information, online at: https://pubs.usgs.gov/periodicals/mcs2021/mcs2021-stone-crushed.pdf, 2022; accessed on December 20, 2022.

United Nations Framework Convention on Climate Change (UNFCCC), 2015.

Vakilifard, N., Kantzas, E. P., Edwards, N. R., Holden, P. B., and Beerling, D. J.: The role of enhanced rock weathering deployment with agriculture in limiting future warming and protecting coral reefs, Environ. Res. Lett., 16, 094005, https://doi.org/10.1088/1748-9326/ac1818, 2021.

Voosen, P.: Ocean geoengineering scheme aces its first field test, News From Science, https://doi.org/10.1126/science.adg3427, December 16, 2022; accessed on December 20, 2022

Wang, H., Pilcher, D. J., Kearney, K. A., Cross, J. N., Shugart, O. M., Eisaman, M. D., and Carter, B. R.: Simulated impact of ocean alkalinity enhancement on atmospheric CO2 removal in the Bering Sea, Earth's Future, e2022EF002816, https://doi.org/10.1029/2022EF002816. Accepted, 2022.

Wright, R. F.: Chemistry of Lake Hovvatn, Norway, Following Liming and Reacidification, Can. J. Fish. Aquat. Sci., 42, 1103–1113, https://doi.org/10.1139/f85-137, 1985.

Zhang, S., Planavsky, N. J., Katchinoff, J., Raymond, P. A., Kanzaki, Y., Reershemius, T., and Reinhard, C. T.: River chemistry constraints on the carbon capture potential of surficial enhanced rock weathering, Limnology and Oceanography, 67, S148–S157, https://doi.org/10.1002/lno.12244, 2022.

https://doi.org/10.5194/egusphere-2022-1505
Preprint. Discussion started: 5 January 2023

Tables

Table 1. Baseline total alkalinity (μmol kg^{-1}) determined at the N. Macapa gateway at the Amazon River mouth during September 2011 and July 2012 (Mu et al., in revision). The means represent the river's alkalinity endmember in that month.

Sample No.	Total Alkalinity (μmol kg^{-1})	
	September 2011	**July 2012**
1	279.8	362.3
2	286.8	322.2
3	310.8	301.2
4	296.3	327.7
5	307.5	296.9
6	275.5	295.8
Mean (std)	**292.8 (14.5)**	**317.7 (25.7)**

Table 2. Summary table for air-sea CO_2 flux in the Amazon River plume and the mass of $CaCO_3$ mineral required for each TA perturbation size (ΔTA) in each month. Positive fluxes indicate CO_2 outgassing and negative fluxes (–) indicate ocean CO_2 uptake. Note that the post-perturbation CO_2 flux and $CaCO_3$ demand increase linearly with increase in ΔTA.

		September 2011			July 2012		
		CO_2 flux		$CaCO_3$	CO_2 flux		$CaCO_3$
		mmol m^{-2} d^{-1}	MtCO$_2$ mo^{-1}	Mt mo^{-1}	mmol m^{-2} d^{-1}	MtCO$_2$ mo^{-1}	Mt mo^{-1}
ΔTA (μmol kg^{-1})	**0**	-0.43	-0.47	0	0.26	0.24	0
	10	-0.46	-0.50	0.2	0.20	0.19	0.3
	20	-0.49	-0.54	0.4	0.15	0.14	0.7
	50	-0.60	-0.65	1.1	-0.02	-0.01	1.7
	100	-0.76	-0.83	2.2	-0.27	-0.26	3.5

Table 3. Theoretical aragonite saturation state (Ω_A) at the surface of the Amazon River-ocean continuum, calculated from the river-ocean mixing model (see Section 2.1 and Figure 2) for different TA perturbation strengths (ΔTA) at various salinities in September 2011 using constant water temperature of 29 °C, according to the equation $\Omega_A = [Ca^{2+}][CO_3^{2-}] / K_{sp}^A$. $[CO_3^{2-}]$ is derived from theoretical TA and DIC in the river-ocean endmember mixing model; the temperature- and salinity- dependent stoichiometric solubility product for aragonite, K_{sp}^A, is calculated from Mucci (1983).

ΔTA	Ω_A(at various salinities)					
μmol kg^{-1}	S=0	S=5	S=10	S=20	S=30	S=35
0	0.0	0.1	0.5	1.8	3.2	3.9
20	0.0	0.1	0.7	2.1	3.5	4.1
50	0.0	0.3	1.0	2.4	3.8	4.4
100	0.1	1.0	1.7	3.1	4.4	5.0
200	2.9	2.6	3.1	4.4	5.7	6.2
260	5.1	3.7	4.0	5.2	6.4	7.0

https://doi.org/10.5194/egusphere-2022-1505
Preprint. Discussion started: 5 January 2023

Figures

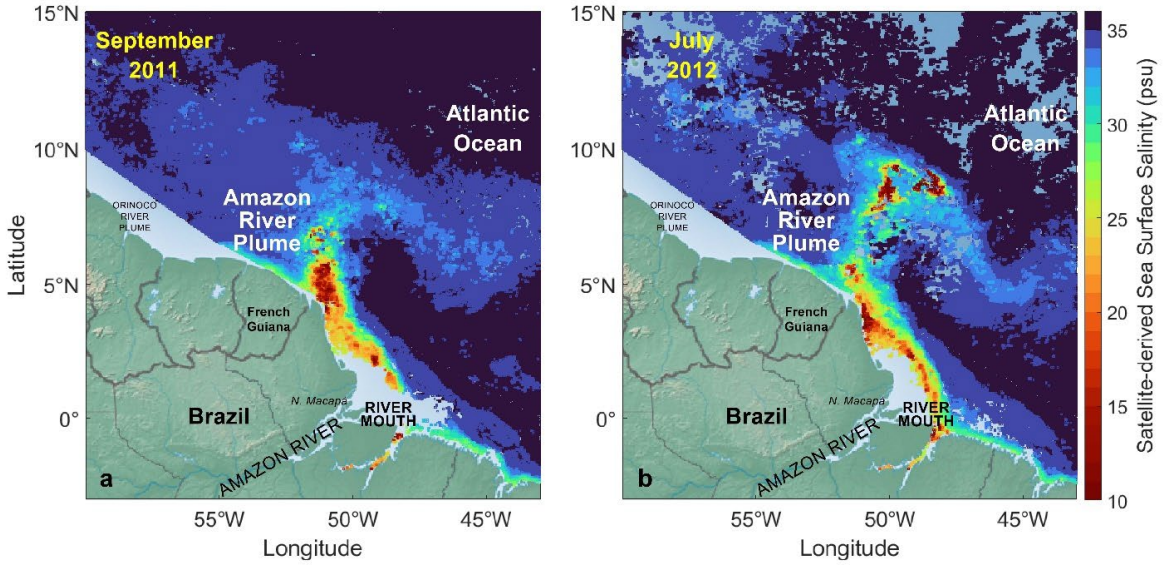

Figure 1. Sea surface salinity (SSS) for the Amazon River plume (15°N–3°S, 43–60°W) during (**a**) September 2011, and (**b**) July 2012, derived from remotely sensed diffuse attenuation coefficient at 490 nm. Area likely affected by the Orinoco River plume (< 150 km off the coastline between 55–60°W) is excluded from this study. Oceanic regions in light blue on the maps indicate the satellite-derived SSS data are unavailable, mostly due to muddy nearshore waters or clouds. See Mu et al. (2021) for further details.

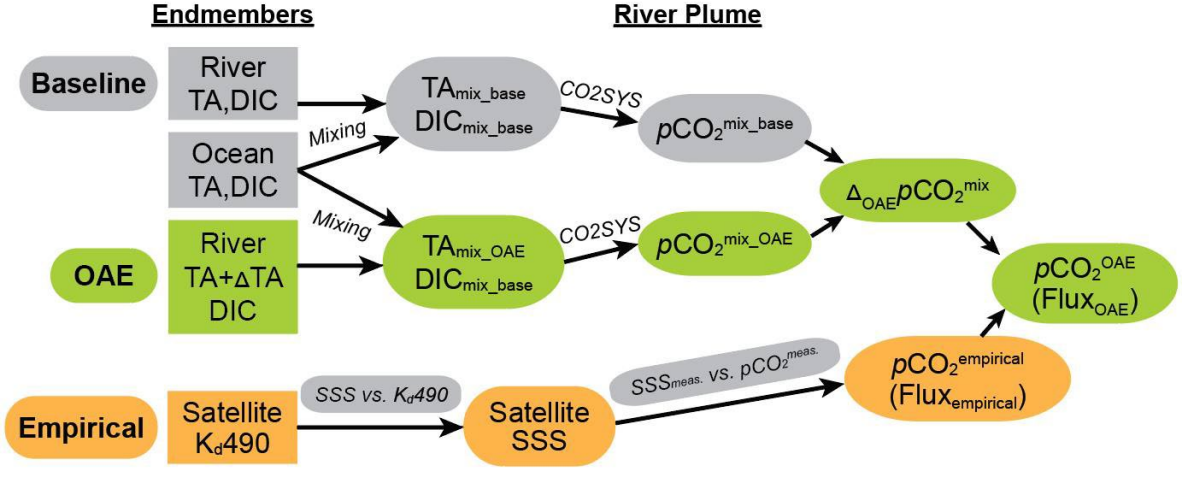

Figure 2. Schematic diagram for the method used to calculate carbonate chemistry and air–sea CO_2 fluxes before and after a hypothetical alkalinity addition (OAE) in the Amazon River-ocean continuum. The baseline and OAE pathways (gray and green) use the conservative mixing model (Equations 3-6) and CO2SYS to calculate the baseline and hypothetical OAE pCO_2. The difference between the baseline and OAE mixed models ($\Delta_{OAE}pCO_2^{mix} = pCO_2^{mix\_OAE} - pCO_2^{mix\_base}$) is added to the empirically-derived pCO_2 at every SSS. The resulting pCO_2^{OAE} is used to calculate the air-sea CO_2 flux across the surface of the plume for each hypothetical OAE experiment.

https://doi.org/10.5194/egusphere-2022-1505
Preprint. Discussion started: 5 January 2023

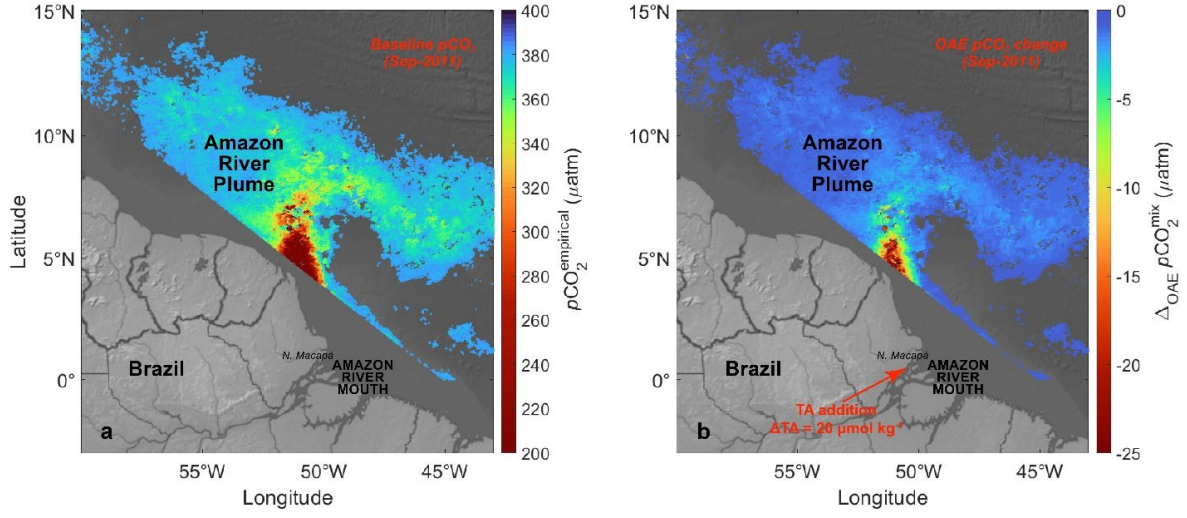

Figure 3. pCO_2 at the surface of the Amazon River plume and its predicted response to alkalinity addition based on satellite-derived SSS. (**a**) Spatial distribution of unperturbed $pCO_2^{empirical}$ (μatm) at the surface of the Amazon River plume ($15 < SSS < 35$) during September 2011, with SSS outside of the plume range removed from this map as the remotely sensed K_d490 vs SSS regression is sufficiently robust only when $15 < SSS < 35$. (See Figure 2 and Section 2.2 for details on how the mapped quantity is defined, and Mu et al. (2021) for additional details). (**b**). Predicted changes in the plume surface pCO_2 (i.e., $\Delta_{OAE}pCO_2^{mix}$ from Equation 9) due to addition of 20 μmol kg^{-1} of alkalinity at the Amazon River mouth during September 2011.

https://doi.org/10.5194/egusphere-2022-1505
Preprint. Discussion started: 5 January 2023

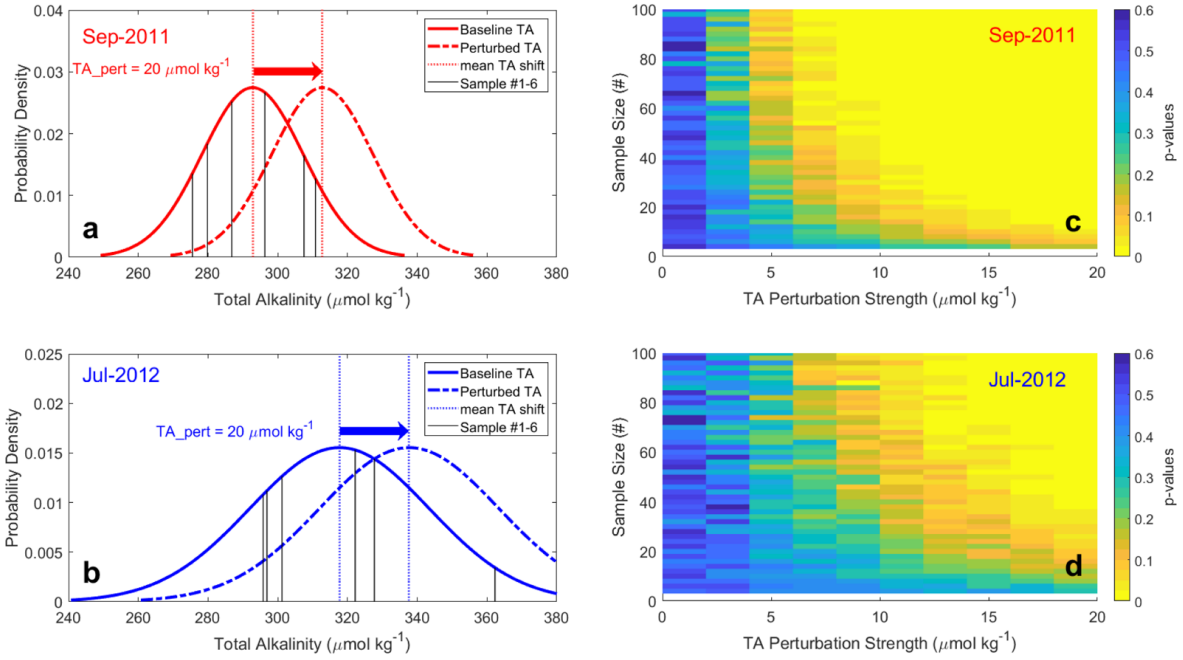

Figure 4. Detectability of hypothetical TA enhancement relative to background variability. (**a**)(**b**). The theoretical shift of TA (μmol kg^{-1}) means and distributions for September 2011 and July 2012 due to the addition of 20 μmol kg^{-1} of TA at the Amazon River mouth. Black lines indicate the *in situ* TA measurements at the mouth on which the baseline data distributions are based. The standard deviations in the perturbation scenarios are assumed the same as those from the baseline. (**c**)(**d**). The p-value maps from t-tests performed between the baseline and TA perturbation scenarios at various sample sizes and TA perturbation strengths for September 2011 and July 2012. Areas in yellow ($p < 0.1$) indicate conditions where an analyst would conclude that the TA perturbation was detected relative to the baseline condition with 90% certainty.

https://doi.org/10.5194/egusphere-2022-1505
Preprint. Discussion started: 5 January 2023

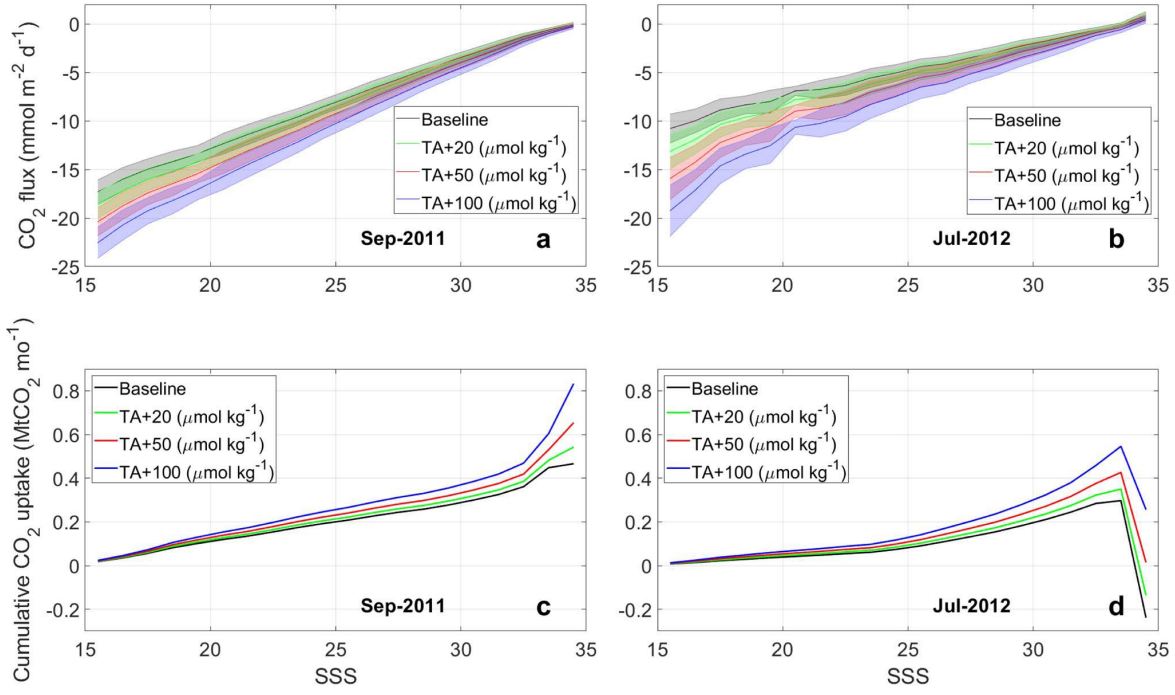

Figure 5. The impact of TA addition on ocean uptake of CO_2 across the Amazon River plume. (Top) Air-sea CO_2 flux density (mmol m^{-2} d^{-1}) in the Amazon River plume at different sea surface salinities for the baseline and multiple TA perturbation scenarios in **(a)** September 2011 and **(b)** July 2012. Standard deviations of the fluxes within each salinity band (1 psu apart) are represented by the shaded areas. Negative values indicate atmospheric CO_2 sinks. (Bottom) Cumulative ocean CO_2 uptake ($MtCO_2$ mo^{-1}) in the Amazon plume due to TA additions in **(c)** September 2011 and **(d)** July 2012. SSS ranging between 15 and 35 is used while SSS < 15 and > 35 is omitted, because the remotely sensed K_d490 vs SSS regression is sufficiently robust only when 15 < SSS < 35 according to the Amazon River plume definition from Mu et al. (2021).